Mechanisms of particle deposition in a fully developed turbulent open channel flow

Chidambaram Narayanan and Djamel Lakehal[a)]
Institute of Energy Technology, Swiss Federal Institute of Technology, ETH-Zentrum/CLT, CH-8092 Zurich, Switzerland

Lorenzo Botto and Alfredo Soldati
Dipartimento di Energetica e Macchine, Universita' degli Studi di Udine, Udine 33100, Italy

(Received 13 August 2002; accepted 17 December 2002; published 3 February 2003)

Particle dispersion and deposition in the region near the wall of a turbulent open channel is studied using direct numerical simulation of the flow, combined with Lagrangian particle tracking under conditions of one-way coupling. Particles with response times of 5 and 15, normalized using the wall friction velocity and the fluid kinematic viscosity, are considered. The simulations were performed until the particle phase reached a statistically stationary state before calculating relevant statistics. For both response times, particles are seen to accumulate strongly very close to the wall in the form of streamwise oriented streaks. Deposited particles were divided into two distinct populations; those with large wall-normal deposition velocities and small near-wall residence times referred to as the *free-flight* population, and particles depositing with negligible wall-normal velocities and large near-wall residence times (more than 1000 wall time units), referred to as the *diffusional deposition* population. Diffusional deposition (deposition induced by the small residual turbulent fluctuations near the wall) is found to be the dominant mechanism of deposition for both particle response times. The free-flight mechanism is shown to gain in importance only for $\tau_p^+ = 15$ particles. For $\tau_p^+ = 5$ particles only 10% deposit because of free flight, whereas the fraction is around 40% for $\tau_p^+ = 15$ particles. This result runs counter to the widely held opinion that free flight is the dominant mechanism of deposition in wall-bounded flows and clearly quantifies the relative importance of the two mechanisms. A simple relationship between the particle wall-normal velocity on deposition and the residence time for free-flight particles is presented. Particle deposition locations over the period of the entire simulation reveal that, while diffusional deposition occurs mostly along streamwise oriented lines below the near-wall particle accumulation patterns, free-flight particles deposit more evenly over the wall.
[DOI: 10.1063/1.1545473]

I. INTRODUCTION

Particle deposition in wall-bounded flows has received considerable attention for more than four decades due to its practical relevance to many industrial applications. One of the earliest models of deposition is the one by Friedlander and Johnstone,[1] who proposed the so-called free-flight theory. The essence of this model is that particles are transported by turbulent motions to within one *stop-distance* of the wall, where they acquire sufficient inertia to coast through the viscous sublayer and deposit. This pioneering model was further improved by the work of many researchers. Cleaver and Yates[2] suggested that the free-flight theory ignores the structure of the near-wall turbulence, and developed a model for the turbulent deposition process which considered the effect of ''sweep'' events in carrying particles to the wall.

Direct numerical simulation (DNS) of a channel flow with Lagrangian particle tracking carried out by McLaughlin[3] showed that particles tend to gradually accumulate in the viscous sublayer and conjectured that this process of accumulation would continue for times much longer than their simulation interval. Some evidence was also provided on the enhancement of particle accumulation due to the addition of the Saffman lift force in the particle equation of motion. However, the time interval of their simulation was too short to obtain reliable results on deposition rates and other Eulerian statistics, as will be clarified later.

Rashidi *et al.*,[4] describing an experiment in which particles were released in an open-channel flow, underlined the importance of sweep-ejection events in depositing and reentraining particles. They too report an accumulation of particles near the wall and observe that particles with radii less than 0.5 wall units, approaching very close to the wall without depositing, are rarely lifted up by wall ejections. The above observations have been confirmed in another experiment conducted by Kaftori *et al.*,[5] where the motion of particles was found to be intimately related to the action of the quasi-streamwise vortices populating the near-wall region. In a recent DNS study, Marchioli and Soldati[6] have helped

[a)]Author to whom correspondence should be addressed. Telephone: +41 (0)1 632 4613; fax: +41 (0)1 632 1166. Electronic mail: lakehal@iet.mavt.ethz.ch

identify the turbulent mechanisms which promote particle accumulation near the wall. They report particle transfer mechanisms due to strong, coherent sweep and ejection events, and specifically point out the effect of small streamwise vortices very close to the wall in promoting particle accumulation under the low-speed streaks. Recently, some attempts to develop empirical models accounting for the near-wall phenomena have been presented.[7]

Brooke *et al.*[8] employed DNS to study particle deposition in a channel flow with the view of evaluating the free-flight theory of Friedlander and Johnstone.[1] By looking at the probability density function (PDF) of the near-wall particle wall-normal velocities, they point out that at any instant only a small fraction of particles have a high enough velocity to execute a free flight to the wall and to deposit. This fact is at odds with the assumption of the original free-flight model, where, at the stop-distance, all particles are supposed to move on a free flight path to the wall.[1] In a subsequent paper, Brooke *et al.*[9] make an interesting subdivision of the particle flux into three components: The free-flight flux, the turbophoretic flux, and the diffusive flux. The turbophoretic flux[10] accounts for the particle flux due to gradients in turbulence intensity, whereas the diffusive flux accounts for the particle flux due to concentration gradients. They found that deposition was dominated by particles starting free flights to the wall at large distances from the wall. However, noting the accumulation of particles near the wall, they mention the possibility of particle deposition due to diffusive processes, even though in their simulation the diffusive deposition flux was reported to be insignificant.

An important point to be noted with regard to the above studies[3,8,9] is the fact that in all simulations the mean particle concentration remained in a state of continuous evolution due to the short simulation times. The wall-normal deposition velocities for most particles was found to be quite high, implying that deposition was predominantly caused by free flight. However, since only a small fraction of the total particle flux directed towards the wall was seen to deposit by free flight,[8] it is natural to expect continued particle accumulation near the wall. In order to reach a steady state under such conditions, some additional mechanism of deposition has to arise to balance the accumulation. Hence, although the diffusive deposition flux was found to be negligible in the above studies, it could become important at later times when a large number of particles have accumulated very close to the wall.

A statement by Brooke *et al.*[9] in this regard acts as the main motivation for the present work. They state that diffusion is not likely to control the deposition flux *at any time* since most of the particles near the wall are trapped in a region of very small wall-normal velocity fluctuations. Very close to the wall, the distance required by a particle to deposit is very small, but the probability of having large enough momentum to carry the particle across that distance is also extremely small. Brooke *et al.*[9] hypothesize that particles residing in the near-wall region would need to move away from the wall in order to acquire a high enough velocity to deposit. Present results for similar particle response times show, to the contrary, that the diffusive flux is the dominant deposition flux.

The present study aims at investigating the mechanisms of particle deposition in the wall region of an open channel flow, using DNS for simulating the flow and Lagrangian particle tracking under the condition of one-way coupling. The focus is on dilute suspensions of particles for which Brownian effects can be ignored, but which interact strongly with the turbulent structures. The study uses the same simulation methodology as van Haarlem *et al.*,[11] who focus in detail on the preferential accumulation phenomenon near the free-slip surface of an open channel, apart from presenting deposition rate coefficients and near-wall variation of particle fluxes. Their method differs from previous numerical work in that it allows the particle field to reach a statistically stationary state by reintroducing deposited particles at the inflow plane. Although the present study follows their work closely, it provides new insight into the mechanisms of particle deposition onto a flat wall for a fully developed particle field. Various conflicting viewpoints exist in the current understanding of deposition mechanisms as pointed out in the previous paragraph. In this work, we clearly show the two dominant mechanisms of deposition and quantify their relative importance.

The outline of the paper is as follows: In the next section we present the governing equations for the fluid and the particle phases, followed by a section describing the numerical methods used and the particle parameters chosen. In the section on results, we present instantaneous particle concentration patterns both near the wall and near the free-slip surface, deposition coefficients, and particle-phase mean and root-mean-square (RMS) velocity profiles, in order to put the present study in perspective with respect to previous ones. The last part of this section is devoted to studying deposition velocity statistics in different ways to bring out the dominant mechanisms of deposition. Conclusions are presented at the end.

II. GOVERNING EQUATIONS

A. Fluid equations

The fluid flow in an open channel is described by the Navier–Stokes equations under the assumptions that the fluid is incompressible, isothermal, and Newtonian. The equations are

$$\frac{\partial u_j}{\partial x_j} = 0, \tag{1}$$

$$\frac{\partial u_i}{\partial t} = S_i - \frac{\partial p}{\partial x_i} + \frac{1}{Re}\nabla^2 u_i, \tag{2}$$

where u_i are the velocity components, $\partial p/\partial x_i$ are the kinematic pressure gradients minus the mean part, and S_i are the nonlinear convective terms minus the mean kinematic pressure gradient. All the variables are normalized by the wall friction velocity u_* and the half height of the domain h. The friction velocity is defined by $u_* = \sqrt{\langle \tau \rangle/\rho}$, where $\langle \tau \rangle$ is the mean shear stress at the wall. No-slip boundary conditions

are imposed at the wall and at the upper boundary free-slip conditions are imposed in order to represent an open channel flow.[12]

B. Particle equations

The motion of particles is described by solving a set of ordinary differential equations for the particle velocity and position at every time instant. Most calculations found in the literature are based on the Maxey and Riley[13] formulation for the force acting on a rigid sphere in a nonuniform flow under the following conditions: The diameter of the sphere is smaller than the Kolmogorov length scale and the sphere is isolated and far from the boundaries (in this manner particle–particle interaction and particle–boundary interaction are excluded). Moreover, the Reynolds number for the relative motion between the particle and the fluid has to be small. The equation for the particle acceleration thus includes the well-known forces such as buoyancy, fluid (due to the pressure gradient and viscous stresses), added-mass, Stokes drag, and Basset forces.

For the case of particles much heavier than the fluid ($\rho_p/\rho \gg 1$), Elghobashi and Truesdell[14] have shown that the only significant forces are the Stokes drag, the buoyancy, and the Basset forces. Moreover, they found that the Basset force was always an order of magnitude smaller than the drag and buoyancy forces. In the present work the effect of gravity is not accounted for either. With the above simplifications the following Lagrangian equation for the particle velocity is obtained

$$\frac{d\mathbf{u}_p}{dt} = -\frac{3}{4}\frac{C_D}{d_p}\left(\frac{\rho}{\rho_p}\right)|\mathbf{u}_p - \mathbf{u}|(\mathbf{u}_p - \mathbf{u}), \tag{3}$$

where C_D is the drag coefficient given by

$$C_D = \frac{24}{Re_p}(1 + 0.15Re_p^{0.687}), \tag{4}$$

in which Re_p is the particle Reynolds number ($Re_p = d_p|\mathbf{u}_p - \mathbf{u}|/\nu$). The empirical correlation[15] for C_D is necessary because Re_p does not necessarily remain small, in particular for depositing particles.[3] For particles strictly in the Stokes regime ($Re_p \ll 1$), Eq. (3) simplifies to

$$\frac{d\mathbf{u}_p}{dt} = -\frac{(\mathbf{u}_p - \mathbf{u})}{\tau_p}, \tag{5}$$

where $\tau_p (= \rho_p d_p^2/18\mu)$ is the particle response time, which is a measure of the time required by a particle released at rest to reach velocity equilibrium with the surrounding fluid.

Other authors[3,16] have also considered the Saffman lift force that could be important near the boundaries. This force acts in the wall-normal direction and is proportional to the wall-normal gradient of the streamwise fluid velocity. Therefore, its contribution might be important near the wall and could influence the particle deposition rate.[3] However, Wang *et al.*[16] in their study of the role of the lift force in particle deposition have found that neglecting the lift force altogether results in only a slight reduction in the deposition rate. Moreover, since many of the previous studies do not account for this term, it has not been included in the present study to facilitate direct comparison.

III. NUMERICAL PROCEDURE

A. Direct numerical simulation of the open channel flow

The fluid equations are solved using a pseudo-spectral method based on Fourier representations in the streamwise and spanwise directions and a Chebychev representation in the wall-normal (nonhomogeneous) direction. For time marching, a two-level explicit Adams–Bashforth scheme was employed for the nonlinear terms and an implicit Crank–Nicholson scheme for the viscous terms. Further details of the numerical procedure can be found in Lam and Banerjee.[12]

The dimensions of the computational domain are chosen to be $l_x = 4\pi h$, $l_y = 2\pi h$, $l_z = 2h$, in the streamwise, spanwise, and normal directions, respectively. In wall units (i.e., normalized using the kinematic viscosity and the friction velocity) the dimensions are $(l_x^+, l_y^+, l_z^+) = (1074, 537, 171)$. A grid consisting of $64 \times 64 \times 65$ nodes was used to perform the computations. A nonuniform distribution of collocation points is used in the normal direction for the Chebychev polynomials, with the grid spacing varying from $\Delta z^+ = 0.10$ near the wall to $\Delta z^+ = 4.19$ in the domain center. The shear Reynolds number of the flow defined as $Re_* = u_* h/\nu$ was chosen to be 85.5. Periodic boundary conditions were imposed in the streamwise and spanwise directions.

B. Lagrangian particle tracking

A Lagrangian particle tracking code[17] has been used to track particles in the flow field. The code interpolates fluid velocities at discrete grid nodes onto the particle position, and with this velocity the equations of motion of the particle are integrated in time.

The code incorporates linear, cubic and fifth-order Lagrangian polynomials for interpolation yielding second, fourth, and sixth-order accuracy, respectively. For the time integration the module has the choice between second and fourth-order Runge–Kutta, and second-order Adams–Bashforth schemes. A parametric study[18] was conducted to choose the appropriate numerical methods for interpolation, integration, and the number of particles needed to obtain accurate statistics. For the simulations presented here, 100 000 particles were tracked using fourth-order Runge–Kutta time integration and fourth-order Lagrangian polynomial interpolation for an interval of 5436 wall time units.

At the start of the simulation, particles were distributed homogeneously over the computational domain. The positions of the particles were chosen randomly and their initial velocity was set equal to the fluid velocity.

1. Particle-phase boundary conditions

When a particle leaves the domain across the outflow plane or in the spanwise direction periodic boundary conditions are applied for both the position and the velocity of the

particle. The wall and free-slip boundaries are considered to be completely absorbing; a particle at a distance less than one particle radius from these boundaries is assumed to have deposited and is removed.

Since the total number of particles has to be maintained constant in time to reach statistically stationary conditions, a particle is reintroduced in the domain at the inflow plane (at $x^+=0$), whenever a particle deposits at the wall or the free-slip boundary. The spanwise and normal coordinates of the reintroduced particle are chosen randomly and their velocity is set equal to the fluid velocity at that position. This procedure introduces a constraint wherein the velocities of the reintroduced particles are necessarily affected by the imposed initial conditions for a certain amount of time.

According to the arguments presented by van Haarlem *et al.*[11] the distance covered by a $\tau_p^+=15$ particle before its velocity becomes independent of the inflow conditions is approximately ten times the height of the channel (which is equivalent to 1700 wall units in the present work). As this length is greater than the streamwise extent of the fluid domain, a longer domain has to be adopted for tracking the particles. The streamwise extent of this domain was set to $5\times l_x$, whereas the spanwise and normal dimensions were kept unchanged. The dimensions of the computational domain in which the particles were tracked were thus, $L_x=5370$, $L_y=537$, and $L_z=171$ in the streamwise, spanwise, and normal directions, respectively. The fluid velocity at every grid point was obtained simply by a periodic extension of the original flow in the streamwise direction. Moreover, only particles located more than 1700 wall units away from the inflow plane were considered for analysis. This method is the same as that used by van Haarlem *et al.*[11]

This procedure offers a twofold advantage: First, it allows the particle-phase to reach a statistically stationary state due to the reintroduction process, and second, particle statistics can be computed as a function of both the wall-normal and the streamwise directions without any effect of the imposed inflow conditions.

C. Particle parameters

Studies on particle deposition suggest that based on the nondimensional particle response times three different regimes of deposition can be defined.[19] For very small particles with $\tau_p^+<0.2$ the deposition rate decreases as τ_p^+ increases. In this regime, particle transport is well represented by a gradient diffusion model accounting for turbulent diffusion in the bulk flow and Brownian diffusion in a thin region adjacent to the wall.

For $0.2<\tau_p^+<20$ a dramatic increase of several orders of magnitude in the deposition rate is observed as the particle time constant increases. This regime is referred to as the *diffusion-impaction* regime, and the observed increase in deposition is mainly due to the strong interaction between particles and the turbulent eddies. In this regime transport of particles due to turbulence plays an important role. In the third regime, known as the *inertia-moderated* regime, particles having very high inertia acquire sufficient momentum from eddies in the turbulent core to reach the wall. Here diffusion plays a very small role and deposition tends to decrease with an increase in the particle time constant, as the response of the particles to the turbulence becomes weaker.[19]

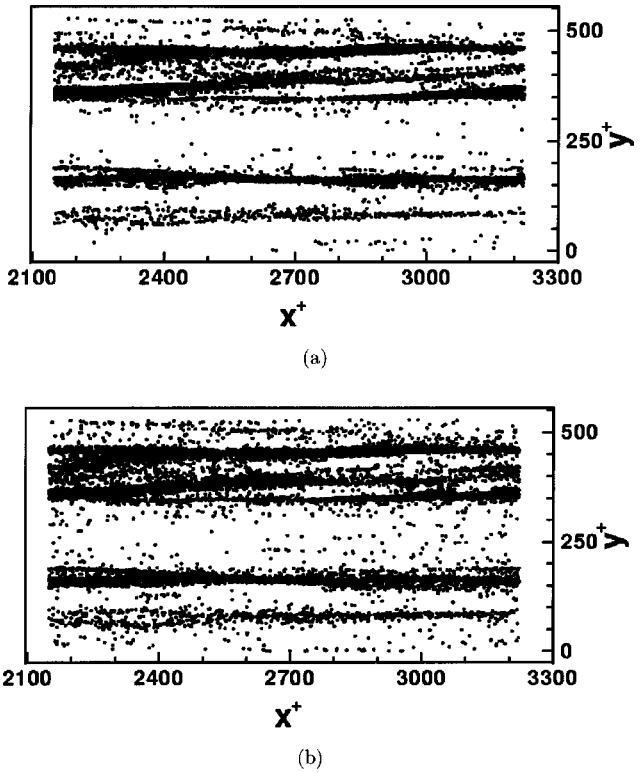

FIG. 1. Particle accumulation patterns near the wall (a) $\tau_p^+=5$, (b) $\tau_p^+=15$.

Two sets of particles with $\tau_p^+=5$ and 15 belonging to the diffusion-impaction regime have been chosen in this study, since the aim is to understand the contribution of turbulence to particle deposition. The values are the same as those studied by van Haarlem *et al.*[11] and have been chosen to facilitate comparison.

IV. RESULTS AND ANALYSIS

A. Preferential concentration

The phenomenon of preferential concentration of particles is one of the most important aspects of this problem. Several animations and snapshots of the particle field clearly reveal varied concentration patterns both in the bulk and near the boundaries.

Starting with a uniform distribution, particles quickly assume an inhomogeneous distribution as they start moving towards both boundaries, due to the phenomenon of turbophoresis. This results in the accumulation of particles, particularly in the near-wall region. The accumulation process continues for a long time until a sharp peak in the concentration is formed in the near-wall region, as shown in the following section. Also, the distribution of particles near the wall is far from being homogeneous in the spanwise direction. The particles, in fact, accumulate in streamwise-oriented streaks. Instantaneous correlation between particle streaks near the wall and the low-speed streaks in a turbulent

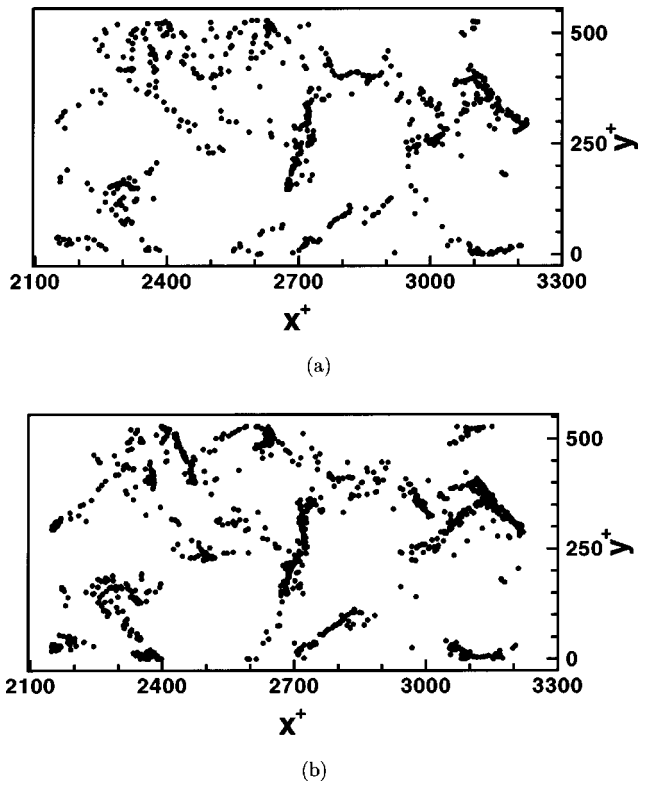

FIG. 2. Particle accumulation patterns near the free surface (a) $\tau_p^+=5$, (b) $\tau_p^+=15$.

boundary layer has been established previously.[4–6,11] Instantaneous near-wall particle concentration patterns are shown in Fig. 1 for both particle response times, for $z^+<3$. Both sets of particles strongly accumulate in streamwise streaks.

Once the particles reach the region near the free-slip boundary, they are subjected to the large-scale structures characteristic of free-surface turbulence such as upwellings, down-drafts, and attached vortices.[11] Typical particle concentration snapshots near the free surface ($z^+>150$) are shown in Fig. 2. Particles are distributed in the form of roughly circular and elongated voids surrounded by thin regions of high concentration, very similar to those obtained by van Haarlem *et al.*[11] The behavior of particles near the free surface will not be discussed further, as the study primarily focuses on near-wall deposition mechanisms.

B. Particle concentration profiles

Figure 3 presents the development of particle number concentration along the streamwise direction. Statistics were obtained by dividing the domain into cross-stream bins of 200 wall units each. The mean concentration in each bin is normalized by the concentration in the case of uniform particle distribution over the entire domain. As expected, the concentration shows an overall decreasing trend which accounts for particle deposition at both boundaries. A discrepancy can be observed at the beginning of the domain, which may be ignored, since the particles there are still affected by the imposed conditions on reintroduction at the inflow plane. The periodic undulations in the concentration, though, require further clarification.

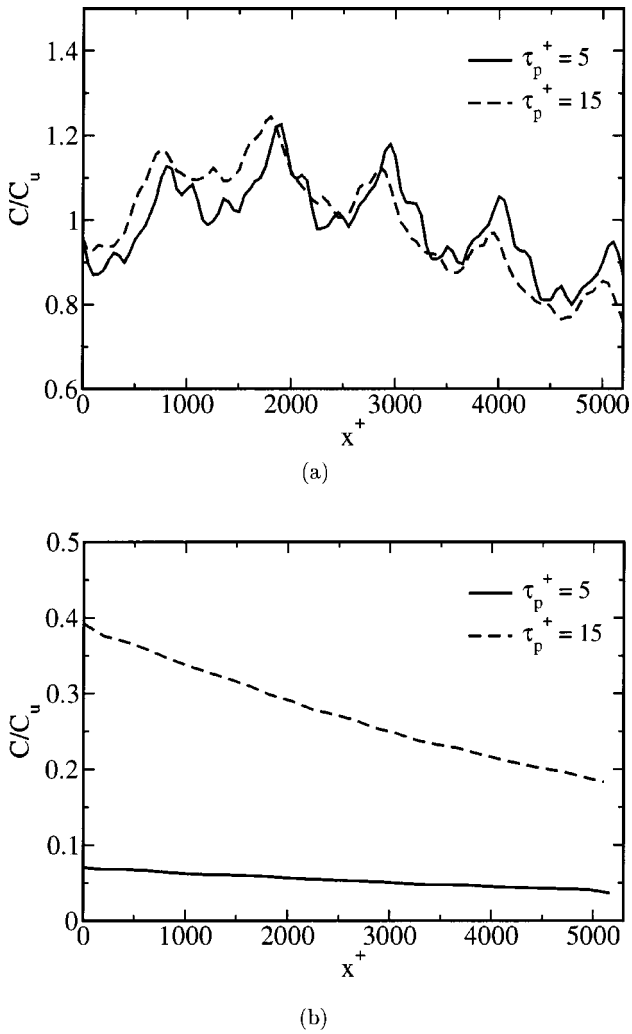

FIG. 3. (a) Streamwise variation of the cross-section averaged concentration, (b) not accounting for particles accumulated very close to the wall ($z^+<3$).

The periodic undulations seen in Fig. 3(a) are an obvious artifact of the periodic extension of the flow domain. Periodic patterns are formed immediately at the start of the simulation and the particles accumulated very close to the wall retain a memory of this fact for a long time due to the quiescent nature of the region and because of their small streamwise velocity. Thus, the actual flow-through time required to wipe out these undulations would be much higher than the current simulation period making it computationally prohibitive. Indeed, in Fig. 3(b), showing the streamwise concentration profile obtained with the procedure described previously, but accounting only for particles located in the region $3<z^+<171$, the profile is almost linear, confirming the observation that the periodic features are mainly due to particle accumulation patterns in the region very close to the wall ($z^+<3$). Figure 3(b) now clearly reveals the difference in the rate of change of bulk concentration between $\tau_p^+=5$ and $\tau_p^+=15$ particles. It points to the fact that $\tau_p^+=15$ particles have a higher overall deposition rate and a higher concentration in the bulk.

The variation of particle concentration along the wall-normal direction at equilibrium (i.e., when the statistically

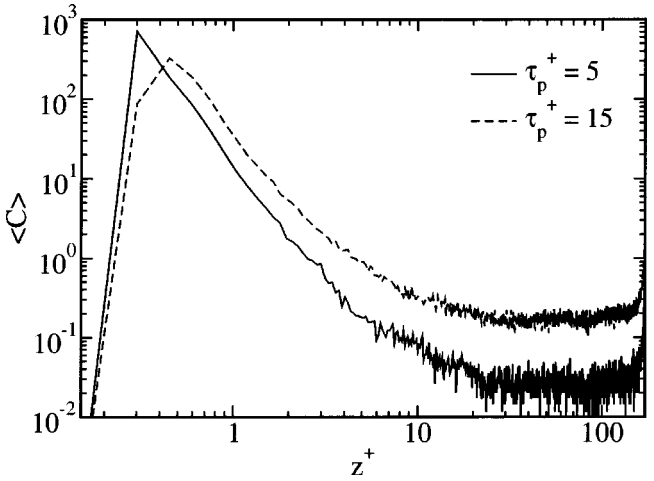

FIG. 4. Average particle concentration profile in the wall-normal direction.

stationary state is achieved; $t^+ > 1000$) is shown in Fig. 4. In this case, the bin height was kept constant at $\Delta z^+ = 0.15$. The distribution shown refers to a region located in the center of the computational domain ($x^+ = 2400-2600$), and the time-averaged concentration in every slab has been normalized by the average concentration of particles in the region considered (i.e., setting the integral across the channel height and width equal to unity). A large increase in particle concentration very close to the wall is observed. Peak values occur at $z^+ = 0.3$ for $\tau_p^+ = 5$ particles and at $z^+ = 0.4$ for $\tau_p^+ = 15$ particles. Particle concentration is higher for $\tau_p^+ = 5$ particles very close to the wall ($z^+ < 0.4$), whereas the opposite is true for $z^+ > 0.4$. This behavior very close to the wall has not been reported in any of the previous studies.

Particle accumulation near the wall has also been observed by other authors[3,4,6,11] in both numerical simulations and experiments. However, a great deal of ambiguity exists between the values and the way the statistics were obtained. In particular, van Haarlem *et al.*,[11] who studied conditions similar to those considered here, do not report such high peaks near the wall for the same particle response times. Their values are of the order of 10, normalized by the initial uniform concentration. This is due to the larger bin size they have used to calculate the average quantities. In fact, their first bin was ten times larger than the one used in the present study. Also, they could not have captured the variation at distances less than one wall unit mentioned in the previous paragraph. In van Haarlem's work, accumulation of particles near the wall is higher for the higher-response-time particles. This trend is confirmed only up to a distance of $z^+ > 0.4$ in the present calculations. Very close to the wall the trend is inverted. A possible scenario to explain this observation is presented below.

Time evolution of the particle concentration (not shown here) indicates clearly that turbophoresis plays an important role in particle dispersion. Since the initial particle distribution is homogeneous, the only mechanism at the beginning capable of inducing a net drift towards the wall is turbophoresis. Referring to the region of maximum particle concentration as the accumulation zone (AZ) and looking at the fluxes towards and away from it at steady state, one can discern a balance between four main contributions: (i) Turbophoresis, where particles migrate from the bulk flow towards the AZ, (ii) free-flight deposition flux, which represents a fraction of the turbophoretic flux passing directly through the AZ and leading to deposition, (iii) *turbulent diffusion* flux acting to smooth the concentration build up in the AZ, and (iv) diffusional deposition flux which again acts to remove particles from the AZ by deposition due to the residual turbulent fluctuations at the AZ. Note that, although in standard parlance the term *turbulent diffusion* accounts for all the above transport mechanisms, here it is specifically meant to signify only the effect of turbulence to smooth out concentration gradients.

Since the deposition of $\tau_p^+ = 5$ particles is mainly due to diffusional deposition (as will be shown later), one would expect the concentration build up required to balance the turbophoretic flux to be higher. Also, the diffusional deposition for $\tau_p^+ = 5$ is less efficient as compared to $\tau_p^+ = 15$ because of the lower level of particle normal-velocity fluctuations at the AZ (refer to Fig. 9). This would strengthen the case for a higher near-wall concentration of $\tau_p^+ = 5$ particles. According to the above scenario, it would be logical to expect a higher concentration very close to the wall for $\tau_p^+ = 5$ particles. However, the situation is quite complicated and a detailed study of the near-wall flux balance would be required to resolve this issue.

It is interesting to note that there is also a slight accumulation of particles at the upper boundary for the cases considered, with values two to three times larger than the bulk concentration. This phenomenon has also been reported by van Haarlem *et al.*[11] and is again attributed to turbophoresis since the free-slip boundary condition generates a gradient in the wall-normal turbulence intensity in the normal direction.

C. Deposition rate

Figure 5(a) shows the cumulative number of particles impinging on the boundaries as a function of time. The slope of the curve reaches an asymptotic value after approximately $t^+ > 1000$. This reflects the fact that after a transient period in which particles redistribute in the domain, the number of particles depositing every instant of time is almost constant. The deposition rate is a strong function of particle inertia, being larger for $\tau_p^+ = 15$ than for $\tau_p^+ = 5$.

The deposition of smaller particles on the wall is remarkably low. The underlying reason is that a large number of these particles reside very close to the wall without depositing and keep continuously accumulating. These particles neither deposit for long times nor are they significantly reentrained in the core flow on reaching the near wall region. This phenomenon was observed by Kaftori *et al.*,[5] and it mainly characterizes experiments with small particles and low shear rate.

The deposition coefficient is defined by

$$K_d^+ = \frac{J_w}{C_m u_*}, \tag{6}$$

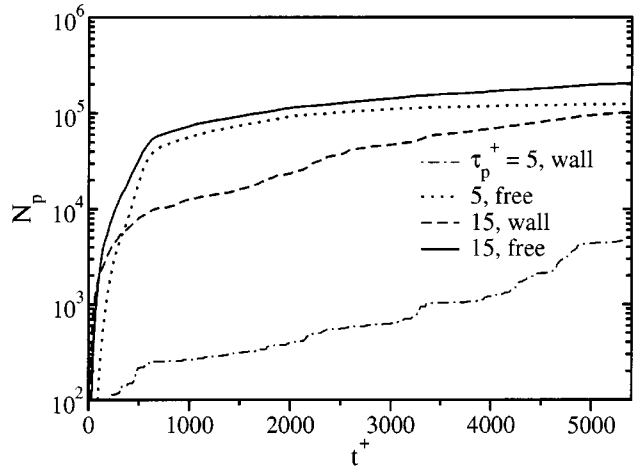

(a)

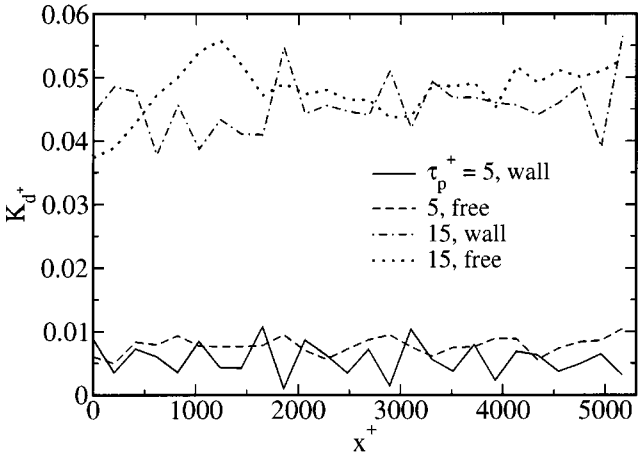

(b)

FIG. 5. (a) Cumulative number of particles deposited at the lower and upper boundaries. (b) Deposition coefficient at the lower and upper boundaries.

where J_w is the mass of particles reaching the surface per unit area per unit time, C_m is the mean bulk concentration of particles, and u_* is the friction velocity. Note that the concentration can alternatively be expressed in terms of number or mass density, as the suspension is mono-disperse.

The nondimensional deposition coefficient is presented in Fig. 5(b) as a function of the streamwise coordinate. Here slabs of $\Delta x^+ = 200$ were used. Tests performed showed that the calculated quantities were actually insensitive to the exact slab thickness. The deposition rate is observed to be rather uniform along the streamwise direction. The deposition rates on the wall are reported in Table I compared to the values found in the literature. The values of the present simulations are in general smaller than those reported in experiments; the comparison shows, for instance, the deposition rate to be three times lower than the data of Liu and Agarwal[20] and 40%–60% lower than those of McCoy *et al.*[21] It can be argued that there is no general agreement among authors on the exact values of the deposition rate. Reportedly, experiments show a wide range of different deposition rates for a given particle response time. For example, one of the key differences could be due to the mean concentration profile existing when the deposition rate was measured. Brooke *et al.*[9] report that in the experiment of Liu and Agarwal[20] droplets were distributed uniformly in a vertical pipe flow. In the present case, the mean profile shows a sharp peak very close to the wall.

TABLE I. Comparison of deposition coefficients from the present study and from previous works.

EXP/DNS	St=5	St=15
McCoy and Hanratty [Exp. (Ref. 21)]	0.0081	0.073
Liu and Agarwal [Exp. (Ref. 20)]	0.015	0.135
van Haarlem *et al.* [DNS (Ref. 11)]	0.0064	0.051
Present (DNS)	0.0056	0.045

Other reasons for the differences could be as follows: The inclusion of the Saffman lift force would enhance deposition as discussed in Sec. II B. Moreover, the near-wall accumulation of particles being very high, other effects, not easily reproducible by numerical simulation, could become important in reality (e.g., particle–fluid interaction or two-way coupling, particle–particle interaction, etc.). Differences in the turbulence properties can also bring about significant changes. In fact, experimental databases have been obtained in physical situations significantly different from those simulated here (e.g., pipe flow at higher Reynolds number).

D. Velocity statistics

1. Mean velocity

Particles having finite inertia accumulate preferentially in the flow both in the bulk and in the near-wall region as discussed in previous sections. Evidently, the particle-phase velocity statistics would not be the same as those of the fluid. Figure 6(a) shows the particle-phase mean streamwise velocity as compared to the fluid. Particle velocity on average is seen to lag behind the fluid. This is surprising for a particle field in equilibrium with the flow, unless one accounts for the preferential concentration of particles in specific regions of the flow which could be characterized by lower average velocities (in this case, the low-speed streaks). A lower particle-phase streamwise velocity was also obtained by Rouson and Eaton[22] in their channel flow simulations for a similar particle response time.

Figure 6(b) shows the mean streamwise velocity obtained by considering the fluid velocity at the particle positions (FVPP) rather than the particle velocities themselves. If the particles were not preferentially distributed in the domain, the profiles for the fluid and FVPP should coincide (to within statistical uncertainty). Therefore, the extent of deviation between these two quantities can be taken as a quantitative estimate of the magnitude of preferential concentration. Figure 6(b) shows that the region with the largest deviation between the particle streamwise velocity and the fluid velocity corresponds to the region with higher preferential concentration. One should also note that particles with $\tau_p^+ = 5$ are slightly more preferentially concentrated than $\tau_p^+ = 15$ particles.

As can be observed in Fig. 6(a), $\tau_p^+ = 15$ particles exhibit a slightly larger mean velocity than $\tau_p^+ = 5$ particles, espe-

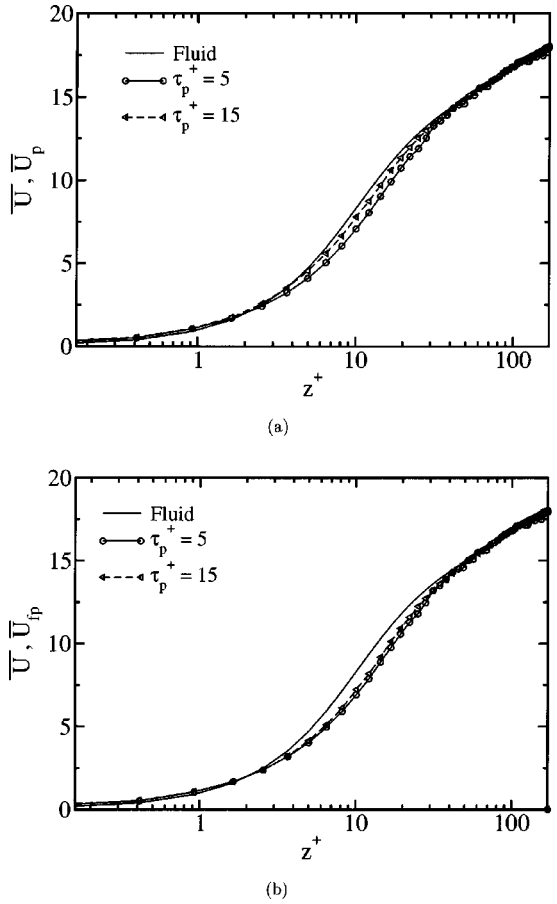

FIG. 6. (a) Mean particle streamwise velocity. (b) Mean streamwise fluid velocity at particle positions.

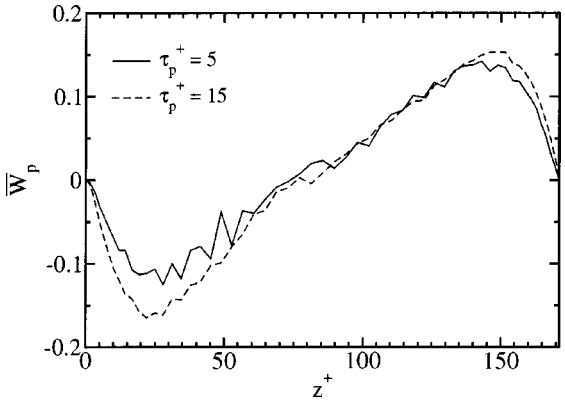

FIG. 7. Mean particle wall-normal velocity.

cially in the region $5<z^+<30$. This behavior has not been noticed in the work of van Haarlem *et al.*[11] In their work, no difference in the mean streamwise velocity was found between the two sets of particles. In reality, since both sets of particles accumulate in the low-speed streaks, a quantitatively lower accumulation would imply a higher mean velocity for the $\tau_p^+=15$ particles.

It is interesting to note that in the experiments of Kaftori *et al.*[23] for smaller response times than in the current study ($\tau_p^+=0.065,0.51,4.41$) the streamwise velocity defect increases with increasing particle response time. Rouson and Eaton[22] obtain similar results as the present study for $\tau_p^+=8.6$ but for larger response times ($\tau_p^+=117$ and 810) the particle streamwise velocity is greater than the fluid velocity (in this case, the gravitational acceleration along the streamwise direction was also considered). The reason for this varied behavior is the dependence of the extent of preferential concentration on the particle response time.

Studies conducted for homogeneous isotropic turbulence[24] show that there exists a critical particle response time which results in maximum preferential accumulation (the value for homogeneous turbulence being of the order of the Kolmogorov time scale). For response times higher and lower than this critical value preferential accumulation is quantitatively lower, which in this particular case would translate into a higher mean velocity. Thus, for increasing particle response times the mean streamwise velocity will first see an increase in the lag up to the critical response time, and from then on a trend in the opposite direction. Therefore, the observed trend in the streamwise velocity would depend on the position of particle response times relative to the critical particle response time. Although it has been shown[22,25] that the Kolmogorov scale remains an appropriate time scale for characterizing preferential concentration for channel flows, a more accurate quantitative estimate for this critical particle response time is not available. As the Kolmogorov scale for inhomogeneous turbulent flows also varies with position, the exact behavior is difficult to quantify without further detailed study.

Figure 7 presents the particle-phase mean wall-normal velocity. Even if the fluid has a zero wall-normal velocity, the particles do have a nonzero wall-normal velocity on average. This is consistent with the fact that for deposition to occur, particles must have a mean drift velocity towards the boundaries. The velocity towards the wall is higher for $\tau_p^+=15$ particles signifying a higher deposition rate. Qualitatively similar results have been presented previously for a pipe flow problem.[19,26] However, since these studies use a Reynolds-averaged approach involving modeling the complex turbulent transport mechanisms in both phases, the results presented here are more reliable and can be looked upon as a validation of previous results. Most of the other studies have not reported the Eulerian particle-phase mean wall-normal velocity which would be very useful for model validation.

2. Turbulence intensity

Turbulence intensity profiles in the streamwise, spanwise, and normal directions are shown in Fig. 8. As can be observed in all cases, particles have a lower fluctuation intensity than the fluid except very close to the wall. The near-wall behavior will be discussed later. A comparison of the results with the data of Brooke *et al.*[9] is satisfactory, whereas the comparison with those of van Haarlem *et al.*[11] is not. However, the fact that the latter authors report RMS values for $\tau_p^+=5$ particles higher than the fluid is difficult to reconcile.

The particle phase turbulence intensity is lower than the fluid due to two mechanisms acting in tandem. The first

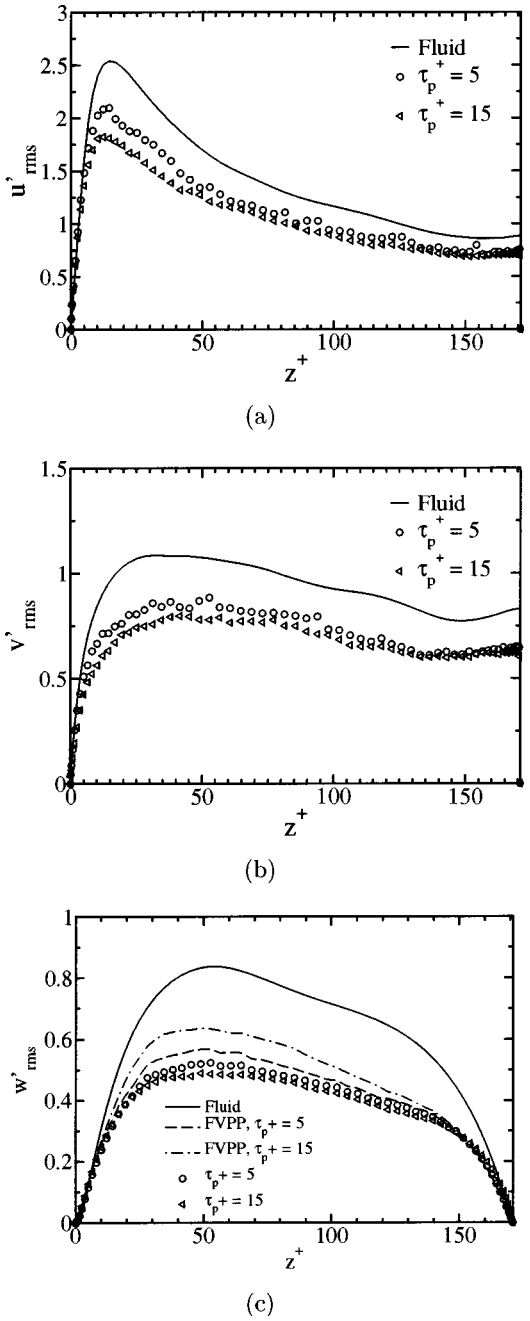

FIG. 8. Particle-phase turbulence intensity, (a) streamwise, (b) spanwise, and (c) wall-normal directions.

mechanism is preferential concentration of particles in regions with lower turbulence intensity (for example, low speed streaks) and the second one is the unresponsiveness of a particle to high frequency or wave number fluid fluctuations due to its inertia. For Stokesian particles in homogeneous turbulence, an expression relating the power spectrum of the particle velocities to that of the fluid velocities can be derived[27]

$$E_p(\omega) = \frac{1}{1+\tau_p^{+2}\omega^2} E_f(\omega), \tag{7}$$

where ω is an angular frequency and E_p and E_f are the particle and the fluid velocity spectra along the particle path, respectively. This expression shows that even in the absence of preferential concentration, the particle fluctuating intensity is suppressed. (We thank one of the reviewers for bringing this point to our attention.) For ease of further discussion, we refer to this effect as *inertial filtering*[27] due to fact that the particle energy spectrum can be obtained from the fluid spectrum through the action of a filtering function. Inertial filtering is the incomplete response of a single particle to its fluctuating fluid environment whereas preferential concentration is related to pattern formation and loses meaning for an isolated particle. Another difference between the two mechanisms is that while the inertial filtering effect increases monotonically with particle inertia, preferential concentration has a more complex dependence on particle inertia. It must be noted that both the above effects are due to the inertia of the particles.

To quantify the contributions of these mechanisms, the fluctuation intensity of the fluid velocities at the particle positions (FVPP) is also presented in Fig. 8(c) along with the particle velocity fluctuation intensity. The fluctuation intensity of FVPP represents the average turbulence intensity felt by the particles and captures the effect of preferential concentration on the particle velocity fluctuation intensity. The figure shows that preferential concentration does cause a large decrease in the particle velocity fluctuation intensity. It shows that $\tau_p^+ = 5$ particles have a higher chance of being in regions of lower turbulence intensity as compared to $\tau_p^+ = 15$ particles. This is consistent with the previous observation that $\tau_p^+ = 5$ particles are more preferentially concentrated than $\tau_p^+ = 15$ particles. Inertial filtering results in a further reduction in the particle velocity fluctuation intensity with respect to the fluctuation intensity of FVPP because of the inability of the particles to respond to the small-scale fluctuations in the surrounding fluid.

The departure of the particle turbulence intensity from the fluctuation intensity of FVPP is again a function of the particle response time. Particles with $\tau_p^+ = 5$ can follow the local fluid turbulent motion better than $\tau_p^+ = 15$ particles. Their turbulence intensity, therefore, is very close to the fluctuation intensity of FVPP, whereas a significant difference between the two quantities exists for $\tau_p^+ = 15$. For large particle response times the reduction in particle turbulence intensity can be attributed mainly to inertial filtering as preferential concentration effects will be small. However, for the response times studied in this work, both the mechanisms play a significant part in reducing the particle turbulence intensity.

Very close to the wall, it can be observed from Fig. 9 that the RMS of particle normal-velocity fluctuations remain nonzero, with $\tau_p^+ = 15$ particles having a significantly higher RMS value as compared to $\tau_p^+ = 5$ particles. This implies that the diffusional deposition process for $\tau_p^+ = 15$ particles would be more efficient.

E. Mechanisms of particle deposition

In this section we first present the cumulative distribution function of particle deposition velocities in Fig. 10(a). Reading from right to left, it indicates the probability that a

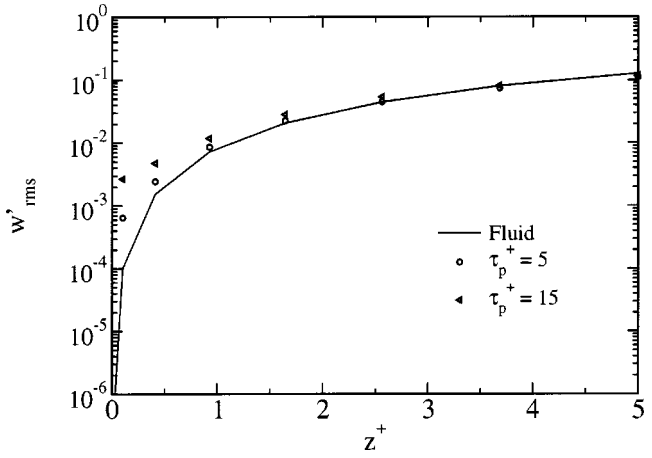

FIG. 9. Near-wall variation of particle wall-normal turbulence intensity.

particle deposits with a velocity higher than the value on the abscissa. A large increase in probability around $-W_p \approx 0.001$ can be observed for both particle response times. The figure suggests the possibility of dividing the population of sampled velocities into two groups: Population A with low deposition velocities, and population B with high velocities.

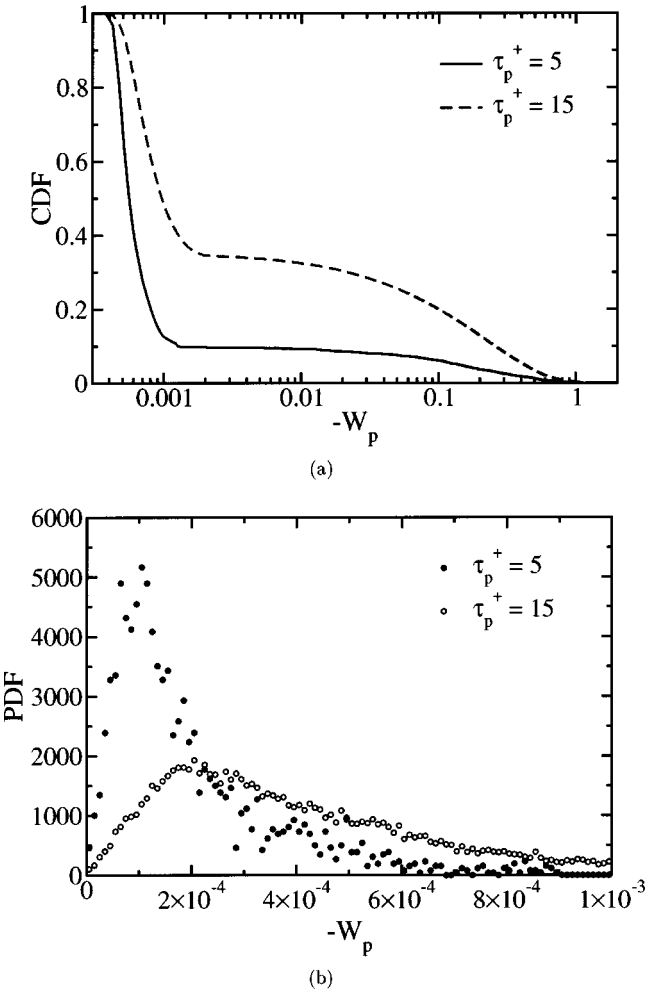

FIG. 10. (a) Cumulative distribution function. (b) Probability density function of wall-normal velocity of depositing particles.

The division is necessarily arbitrary, but the existence of a significant intermediate range of velocities where no deposition occurs (the flat portion of the curves) clearly implies such a separation.

For $\tau_p^+ = 5$ particles almost 90% deposit with velocities smaller than 0.001, and the remaining 10% deposit with velocities greater than 0.1. For $\tau_p^+ = 15$ particles, the corresponding fractions are 60% and 40%, respectively. As mentioned by Brooke *et al.*,[9] particles depositing with a velocity roughly equal to the fluid velocity fluctuations very close to the wall may be said to undergo *diffusional deposition*. On the other hand, particles depositing with velocities much larger than the near-wall velocity fluctuations may be referred to as *free-flight particles*. Using this definition, the present study suggests that once the particle field has reached a statistically steady state, the dominant mechanism of deposition is diffusional. The free-flight population, however, constitutes a significant fraction for $\tau_p^+ = 15$ particles. Figure 10(b) shows the PDF of the normal velocities of the deposited particles. The peaks correspond to velocity values of around 1×10^{-4} for $\tau_p^+ = 5$ particles and of 2×10^{-4} for $\tau_p^+ = 15$ particles, confirming the above fact.

At this point, an interesting comparison can be made between the present study and some of the previous work[3,8,9] mentioned earlier. Brooke *et al.*[9] found that most of the depositing particles have a velocity much higher than the RMS wall-normal velocity near the wall. This led them to conclude that deposition occurs predominantly because of the free-flight process similar to the model proposed by Friedlander and Johnstone.[1] They also found that the number of particles depositing by diffusion is small and that the diffusion flux is negligible. Thus, their conclusions run exactly counter to the results obtained in the present study. This fact is also observed in the probability density function [Fig. 10(b)], where, in the case of Brooke *et al.*,[9] the value of the most probable deposition velocity is around 1000 times larger for similar particle response times. This is understandable because, in their simulation, free flight was the only observed mechanism of deposition.

The reason for this drastic discrepancy lies in the differences between the simulation procedures. In their work, approximately 16 000 particles were released from a plane at $z^+ = 40$ and were tracked for 700 wall time units. The deposited particles were removed and not reintroduced into the flow, thus precluding the possibility of achieving a statistically stationary state. Also, given the short simulation time, they report that the mean concentration profile continues to evolve throughout the simulation. In the present study, the simulation was carried out for more than 5000 wall time units, so that an acceptable steady state was reached for the calculation of the deposition coefficient [refer to Fig. 5(a)]. At steady state, the concentration near the wall becomes high enough for diffusional deposition to be dominant. Since only a small fraction of the particles arriving near the wall have large enough velocities to deposit by free flight,[8] a steady state can be reached only by an increase in diffusional deposition. Although this process of deposition is not very efficient because of the quiescent environment close to the wall, it is aided by the large accumulation of particles very close to

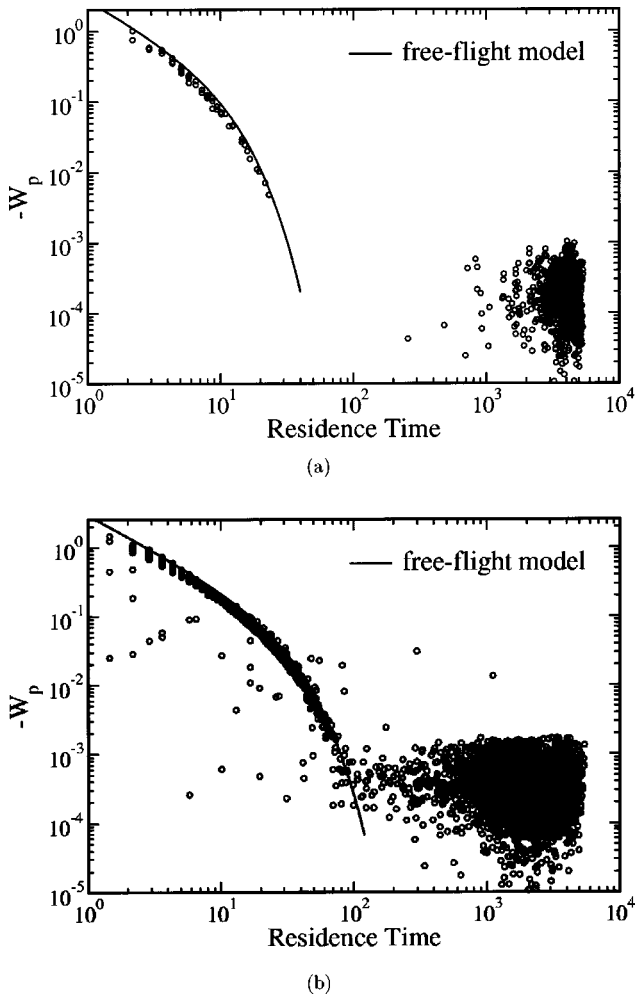

FIG. 11. Residence time of particles in the slab $z^+<3$ versus deposition velocity for (a) $\tau_p^+=5$, (b) $\tau_p^+=15$.

the wall. Moreover, a lower concentration away from the wall results in a reduction in the number of possible free-flight particles.

To analyze this claim further, a particle residence time analysis has been conducted. The time spent by a particle before deposition in a slab 3 wall units from the wall has been recorded. An algorithm was implemented such that, if a particle escapes from the slab before depositing (due to re-entrainment), the time counter for this particle was reinitialized to zero. Figure 11 shows a scatter plot of the particle residence time versus the particle wall-normal velocity on deposition. The two populations of diffusional and free-flight particles can now be distinguished more clearly in combination with the residence time. The free-flight population can now be defined as particles having both a high deposition velocity and a short residence time, and the diffusional deposition particles are those with very small deposition velocities and very large residence times. Logarithmic scales have been deliberately adopted to clearly show the separation between the two different populations.

1. Free-flight mechanism

The behavior of the deposition velocity versus residence time shown for the free-flight particles in Fig. 11 can be explained using a very simple analysis. Assuming that the particle wall-normal velocity is much larger than the wall-normal fluid velocity fluctuations in the near-wall region ($z^+<3$ for the residence time analysis), the equation for the particle wall-normal velocity can be approximated by

$$\frac{dW_p}{dt}=-\frac{W_p}{\tau_p^+}, \tag{8}$$

the solution of which is obtained as

$$W_p=W_{p,[z^+=3]}\exp\left(\frac{-t}{\tau_p^+}\right). \tag{9}$$

The wall-normal velocity at deposition, W_{dep}, therefore is

$$W_{\mathrm{dep}}=W_{p,[z^+=3]}\exp\left(\frac{-t_{\mathrm{res}}}{\tau_p^+}\right), \tag{10}$$

where t_{res} is the residence time of the particle. Solving for the position of the particle such that $z^+=3$ at $t^+=0$ and $z^+=0$ at $t^+=t_{\mathrm{res}}$, the following condition is obtained:

$$3=W_{p,[z^+=3]}\tau_p^+\left[\exp\left(\frac{-t_{\mathrm{res}}}{\tau_p^+}\right)-1\right]. \tag{11}$$

Eliminating $W_{p,[z^+=3]}$ from Eqs. (10) and (11), a relationship between t_{res} and W_{dep} is obtained

$$\tau_p^+ W_{\mathrm{dep}}\left[1-\exp\left(\frac{t_{\mathrm{res}}}{\tau_p^+}\right)\right]=3, \tag{12}$$

where the number 3 on the right-hand side is the slab height chosen for the residence time analysis.

This expression matches very well the actual behavior obtained by the DNS for particles with $\tau_p^+=5$ as well as 15, as shown in Fig. 11. As the velocity of the particles entering the slab becomes smaller and comparable to the RMS fluid velocity in the region (<0.01), it is no longer appropriate to neglect the effect of the fluid velocity fluctuations on the particle path, and the assumption of free flight breaks down. Particles now do not have sufficient momentum to deposit directly and remain in the slab for longer periods of time until they deposit by a random process due to the residual fluctuations near the wall.

2. Preferential deposition

Another interesting statistic is the location where particles tend to deposit on the wall. At every time step, only a few particles deposit, hence no preferential zones can be discerned when taking instantaneous snapshots of deposition locations. Figure 12 shows the locations where particles have deposited on the wall over the whole simulation interval. This can be considered as the probability that a particle deposits at a certain position on the wall. In the figure, the diffusional deposition population is shown in gray.

An examination of the distribution leads to the conclusion that the diffusional deposition population deposits preferentially in streamwise oriented streaks, while the free-flight ones are more evenly distributed over the whole plane. This is not surprising, since diffusional deposition particles come from locations very close to the wall, where particles have

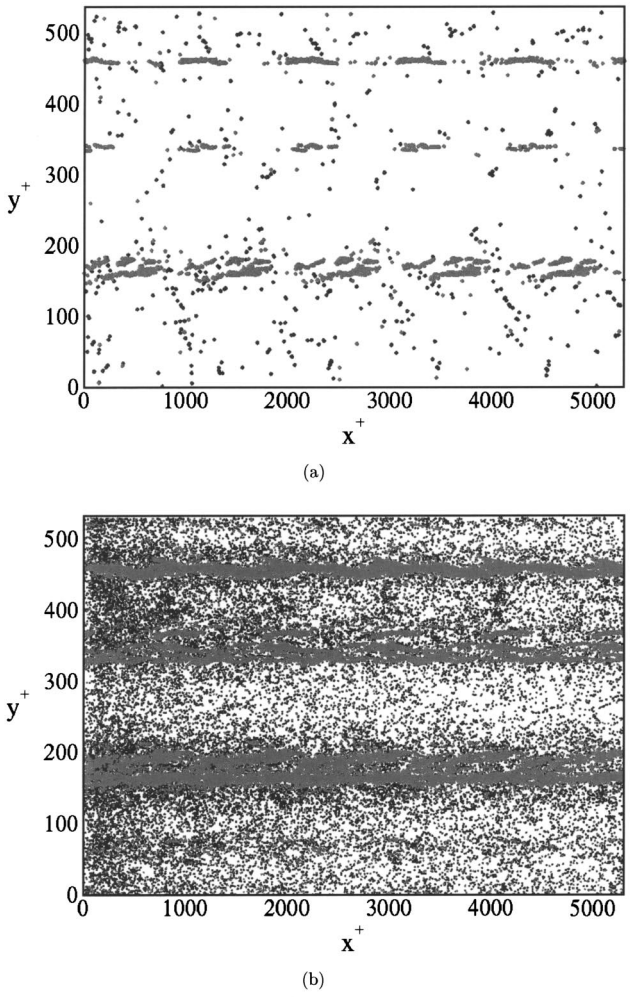

FIG. 12. Particle deposition patterns, (a) $\tau_p^+ = 5$, (b) $\tau_p^+ = 15$.

already accumulated in such streaks. These near-wall streamwise particle streaks have a long lifetime because they exist very close to the wall in a particularly quiescent region, and move with very small streamwise velocity. Consequently, particle distribution at the deposition position clearly reflect the near-wall particle distribution. On the other hand, free-flight particles arrive from regions further away from the wall, where larger scale fluid motions project particles more evenly towards the wall. This result has not been presented in previous studies.

V. SUMMARY AND CONCLUSIONS

Direct numerical simulation of a turbulent open channel flow was combined with Lagrangian particle tracking to study the mechanisms of particle deposition onto the wall. Particles with inertial response times of 5 and 15 were tracked under the assumption of one-way coupling. The Stokes drag force, corrected for higher particle Reynolds numbers, was assumed to be the only force acting on the particles. Particles were removed on coming within one radius of the boundaries and reintroduced at the inflow plane at a random location. This procedure allowed the eventual development of a statistically stationary particle field.

Particle concentration patterns were found to reflect the flow characteristics in the different regions of the flow. Near the wall, particles accumulate in streamwise oriented streaks correlated with the so-called low-speed streaks in wall turbulence. Near the free-slip boundary they form large circular and elongated voids surrounded by thin regions of high concentration, consistent with the large scale structure of turbulence near a free surface. A large increase in particle concentration very close to the wall is observed. The peak value is located around $z^+ \approx 0.3-0.4$. This flux of particles towards the wall is driven by the process of turbophoresis. Very close to the wall, particle concentration is higher for $\tau_p^+ = 5$ particles than for $\tau_p^+ = 15$ particles.

The deposition rates presented in the paper compare reasonably well with nominal experimental and numerical results presented previously. The deposition rate for $\tau_p^+ = 15$ particles was found to be significantly higher than for $\tau_p^+ = 5$ particles. The particle-phase mean streamwise velocity is shown to be smaller than that of the fluid for both sets of particle response times. This is attributed to the accumulation of particles in the low-speed regions of the flow. Preferential concentration was quantified by examining the mean streamwise velocity of the fluid at the particle positions. The results show that $\tau_p^+ = 15$ particles are slightly less preferentially concentrated in the region $5 < z^+ < 30$. The particle-phase mean wall-normal velocity is nonzero, even though the fluid has zero mean wall-normal velocity. The velocity towards the wall was found to be higher for $\tau_p^+ = 15$ particles, consistent with their higher deposition rate. The particle phase turbulence intensity was found to be significantly lower than the fluid phase due to two mechanisms working in conjunction with each other. The first mechanism is the preferential concentration of particles in regions with lower turbulence intensity and the second one is the lack of response of a particle to small-scale turbulent fluctuations due to its inertia.

Studies on particle deposition had so far indicated that free flight is the dominant mechanism for particle deposition in wall-bounded flows. One of the main findings of this study is the fact that diffusional deposition (deposition induced by the small residual turbulent fluctuations near the wall) of particles strongly concentrated near the wall is the dominant mechanism for particle deposition. This is clearly suggested by the cumulative distribution functions of the wall-normal velocities of depositing particles. Almost 90% of the $\tau_p^+ = 5$ particles deposit due to this mechanism. The free-flight mechanism is shown to gain in importance for $\tau_p^+ = 15$, where it accounts for 40% of the deposited particles. This fact is further clarified by looking at the deposition velocity vis-a-vis the residence time of the particles in a thin slab adjacent to the wall before deposition. A clear distinction between diffusional and free-flight particles was revealed. It was also shown that free-flight particles deposit more uniformly over the wall as compared to the diffusional particles that deposit in streamwise oriented streaks coinciding with the near-wall accumulation patterns.

ACKNOWLEDGMENTS

The authors appreciate the help and support of Marco Fulgosi and Professor Yadigaroglu. L.B. gratefully acknowl-

edges the financial support by the Nuclear Engineering Laboratory, ETH-Zurich. Part of the computations were performed on the NEC SX-5 at the Swiss Center for Scientific Computing (CSCS) in Manno, Switzerland.

[1]S. K. Friedlander and H. F. Johnstone, ''Deposition of suspended particles from turbulent gas streams,'' Ind. Eng. Chem. **49**, 1151 (1957).
[2]J. W. Cleaver and B. A. Yates, ''Sublayer model for the deposition of particles from a turbulent flow,'' Chem. Eng. Sci. **30**, 983 (1975).
[3]J. B. McLaughlin, ''Aerosol particle deposition in numerically simulated channel flow,'' Phys. Fluids A **1**, 1211 (1989).
[4]M. Rashidi, G. Hetsroni, and S. Banerjee, ''Particle–turbulence interaction in a boundary layer,'' Int. J. Multiphase Flow **16**, 935 (1990).
[5]D. Kaftori, G. Hetsroni, and S. Banerjee, ''Particle behavior in the turbulent boundary layer. I. Motion, deposition, and entrainment,'' Phys. Fluids **7**, 1095 (1995).
[6]C. Marchioli and A. Soldati, ''Mechanisms for particle transfer and segregation in turbulent boundary layer,'' J. Fluid Mech. **468**, 283 (2002).
[7]M. Shams, G. Ahmadi, and H. Rahimzadeh, ''A sublayer model for deposition of nano- and micro-particles in turbulent flows,'' Chem. Eng. Sci. **55**, 6097 (2000).
[8]J. W. Brooke, K. Kontomaris, T. J. Hanratty, and J. B. McLaughlin, ''Turbulent deposition and trapping of aerosol at the wall,'' Phys. Fluids A **4**, 825 (1992).
[9]J. W. Brooke, T. J. Hanratty, and J. B. McLaughlin, ''Free-flight mixing and deposition of aerosol,'' Phys. Fluids **6**, 3404 (1994).
[10]M. W. Reeks, ''The transport of discrete particles in inhomogeneous turbulence,'' J. Aerosol Sci. **14**, 729 (1983).
[11]B. van Haarlem, B. J. Boersma, and F. T. M Niewstadt, ''Direct numerical simulation of particle deposition onto a free-slip and no-slip surface,'' Phys. Fluids **10**, 2608 (1998).
[12]K. Lam and S. Banerjee, ''On the condition of streak formation in a bounded turbulent flow,'' Phys. Fluids A **4**, 306 (1992).
[13]M. R. Maxey and J. K. Riley, ''Equation of motion for a small rigid sphere in a nonuniform flow,'' Phys. Fluids **26**, 883 (1983).
[14]S. Elghobashi and G. C. Truesdell, ''Direct simulation of particle dispersion in a decaying isotropic turbulence,'' J. Fluid Mech. **242**, 655 (1992).
[15]R. Clift, J. R. Grace, and M. E. Weber, *Bubbles, Drops and Particles* (Academic, New York, 1978).
[16]Q. Wang, K. D. Squires, M. Chen, and J. B. McLaughlin, ''On the role of the lift force in turbulence simulations of particle deposition,'' Int. J. Multiphase Flow **23**, 749 (1997).
[17]C. Narayanan, D. Lakehal, and G. Yadigaroglu, ''Linear stability analysis of particle-laden mixing layers using Lagrangian particle tracking,'' Powder Technol. **125**, 122 (2002).
[18]L. Botto, ''Droplet deposition in turbulent air–water sheared flow,'' M.S. thesis, University of Udine, Italy (2002).
[19]J. Young and A. Leeming, ''A theory of particle deposition in turbulent pipe flow,'' J. Fluid Mech. **340**, 129 (1997).
[20]B. Y. H. Liu and J. K. Agarwal, ''Experimental observation of aerosol deposition in turbulent flow,'' J. Aerosol Sci. **5**, 145 (1974).
[21]D. D. McCoy and T. J. Hanratty, ''Rate of deposition of droplets in annular two-phase flow,'' Int. J. Multiphase Flow **3**, 319 (1975).
[22]D. W. I. Rouson and J. K. Eaton, ''On the preferential concentration of solid particles in turbulent channel flow,'' J. Fluid Mech. **428**, 149 (2001).
[23]D. Kaftori, G. Hetsroni, and S. Banerjee, ''Particle behavior in the turbulent boundary layer. II. Velocity and distribution profiles,'' Phys. Fluids **7**, 1107 (1995).
[24]L. P. Wang and M. R. Maxey, ''Settling velocity and concentration distribution of heavy particles in homogeneous isotropic turbulence,'' J. Fluid Mech. **256**, 27 (1993).
[25]J. R. Fessler, J. D. Kulick, and J. K. Eaton, ''Preferential concentration of particles in a turbulent channel flow,'' Phys. Fluids **6**, 3742 (1994).
[26]S. Cerbelli, A. Giusti, and A. Soldati, ''ADE approach to predicting dispersion of heavy particles in wall-bounded turbulence,'' Int. J. Multiphase Flow **27**, 1861 (2001).
[27]J. O. Hinze, *Turbulence*, 2nd ed. (McGraw Hill, New York, 1975).